Electronic Supplementary Information

High-performance anode-less all-solid-state batteries enabled by multisite nucleation and an elastic network

Jihoon Oh,‡[a,b] Yeeun Sohn,‡[a,b] and Jang Wook Choi*[a,b]

[a] *School of Chemical and Biological Engineering and Institute of Chemical Process, Seoul National University, 1 Gwanak-ro, Gwanak-gu, Seoul 08826, Republic of Korea. E-mail: jangwookchoi@snu.ac.kr*
[b] *Hyundai Motor Group-Seoul National University (HMG-SNU) Joint Battery Research Center (JBRC), Seoul National University, Seoul, Republic of Korea*

† Electronic Supplementary Information (ESI) available: See DOI: 10.1039/x0xx00000x

‡ These two authors contributed equally to this work.

Experimental Section

Preparation of electrode

Mg, Ag, and Sn-based electrodes were fabricated via slurry casting method. The MgAgSn slurry comprised metallic nanopowders—Mg (AVENTION, D50 = 800 nm), Ag (Alfa-Aesar, D50 = 30 nm), and Sn (Sigma-Aldrich, D50 = 150 nm)—in a 2:1:1 weight ratio, blended with 10 wt% binder (Elastane [TK Chemical] or PVDF [Kynar]) dissolved in *N*-methylpyrrolidone (NMP) solvent. Homogenization was achieved using a centrifugal mixer (THINKY Inc.) at 2000 rpm for 5 min. The resultant slurries were cast uniformly onto a stainless-steel (SUS) substrate under ambient conditions, followed by drying at 80 °C for 12 h to achieve a 5 μm thick layer. For full-cell evaluations, the composite cathode was prepared by combining $LiNbO_3$-coated NCM811, LPSCl, vapor-grown carbon fiber (VGCF), and butadiene rubber (BR) binder in a weight ratio of 76:20:2.5:1.5. Using butyl butyrate as the solvent, the mixture was cast onto Al foil and dried at 100 °C for 15 h, resulting in a cathode with an active material loading of 12 mg cm^{-2}.

Characterization of materials

The crystal structures of the metal nanopowders were characterized by XRD analysis (New D8 Advance, Bruker), with characteristic peaks identified using the International Centre for Diffraction Data (ICDD) database. The chemical bonds of the Elastane binder were characterized using FT-IR spectroscopy (Tensor27, Bruker). Morphological analysis of the electrodes was conducted using field emission SEM (FE-SEM, JSM-7800F Prime, JEOL) for top-view imaging and focused ion beam microscopy (FIB, Helios 650, FEI) for cross-sectional examination. Scratch testing (MST3, Anton Paar) was performed by applying a linearly increasing force from 10 mN to 135 mN across a 2 mm distance while recording the penetration depth. Nano-indentation measurements were conducted using an ultra-precision surface mechanical analyzer (Anton Paar, Austria), with the unloading phase initiated upon reaching a fixed indentation depth of 1000 nm. The adhesion force was assessed through 180° peeling tests using a universal testing machine (UTM, QM100s, QMESYS), where 3M Scotch tapes were applied to specimen surfaces and peeled at a constant rate of 10 mm s^{-1} while measuring the peeling force. To evaluate the adhesion properties of the polymer films, Elastane or PVDF

was dissolved in NMP at a concentration of 10 wt% and cast onto a SUS substrate. The resulting polymer electrodes were then dried at 80°C for 12 hours before the peel-off test, with the polymer film thickness controlled to 15 μm.

Electrochemical characterization

The fabrication of all-solid-state half-cells involved a sequential assembly process. Initially, 100 mg of LPSCl was cold-pressed at 120 MPa to form an SE layer with a 10 mm diameter. The anode-less electrode was positioned beneath this SE layer, followed by compression of the assembled components at 390 MPa. Li foil was then placed on top of the SE layer, with SUS foil serving as current collectors for both electrodes. The assembled cell was housed in a case under 20 MPa stack pressure during testing. All-solid-state full-cells were assembled following a similar procedure. The SE layer was fabricated using a cold-pressing method identical to that for the half-cells. The cathode and anode-less electrode were positioned on opposite sides of the SE pellet, followed by compression at 390 MPa. The compressed assembly was placed in a housing case maintained at 20 MPa stack pressure. All assembly procedures were conducted in an argon-filled glove box. Electrochemical evaluations were performed at 25 °C. For half-cell tests, the stripping cutoff voltage was set at 0.1 V using a battery cycler (WBCS 3000, WonATech). Full-cell performance was evaluated in constant current and constant voltage (CC/CV) mode for charging and constant current (CC) mode for discharging, operating within a 2.5–4.2 V potential range using the same battery cycler. Resistance measurements of the all-solid-state half-cells were conducted via EIS using a battery cycler (VSP, Bio-Logic) with scanning frequencies from 1 MHz to 0.1 Hz. In-situ EIS analysis was performed after 3 precycles of half-cell plating-stripping operations.

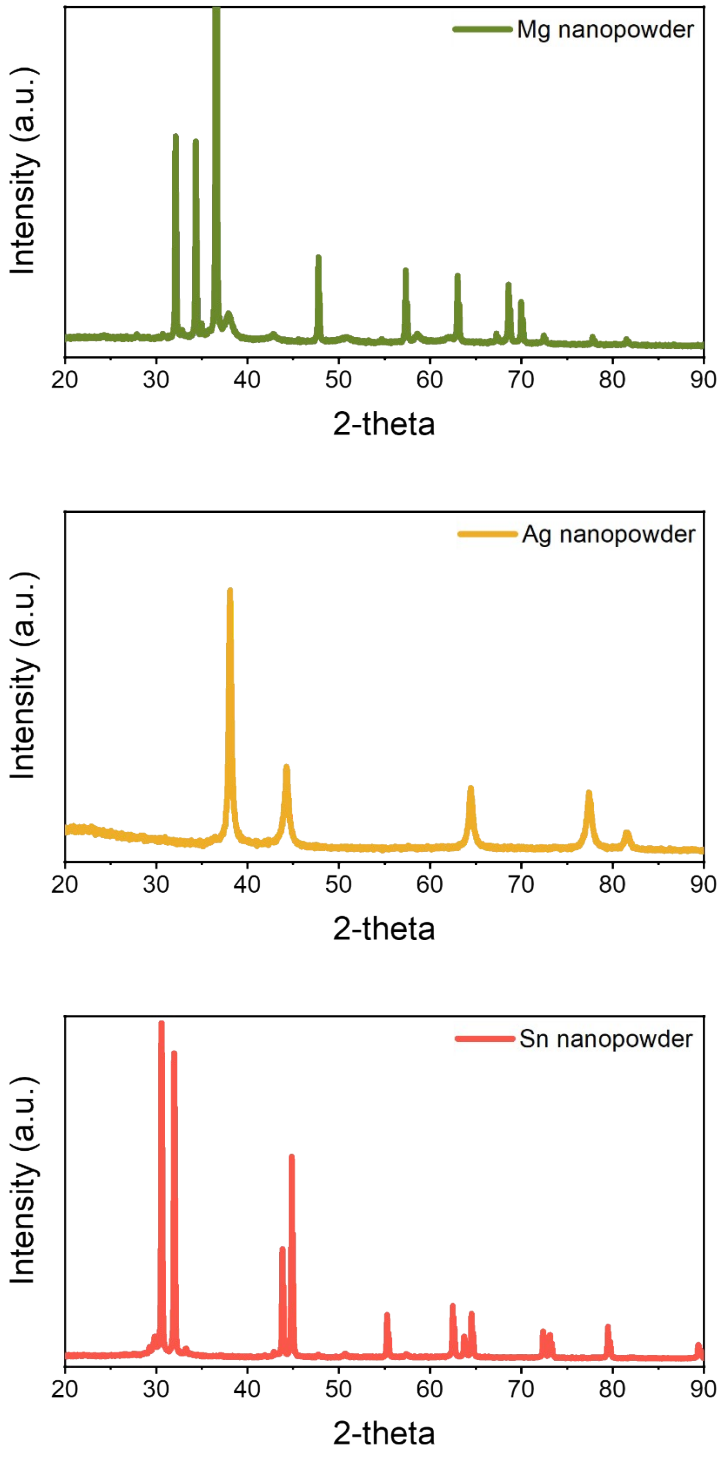

Fig. S1 XRD patterns of the metal nanopowders.

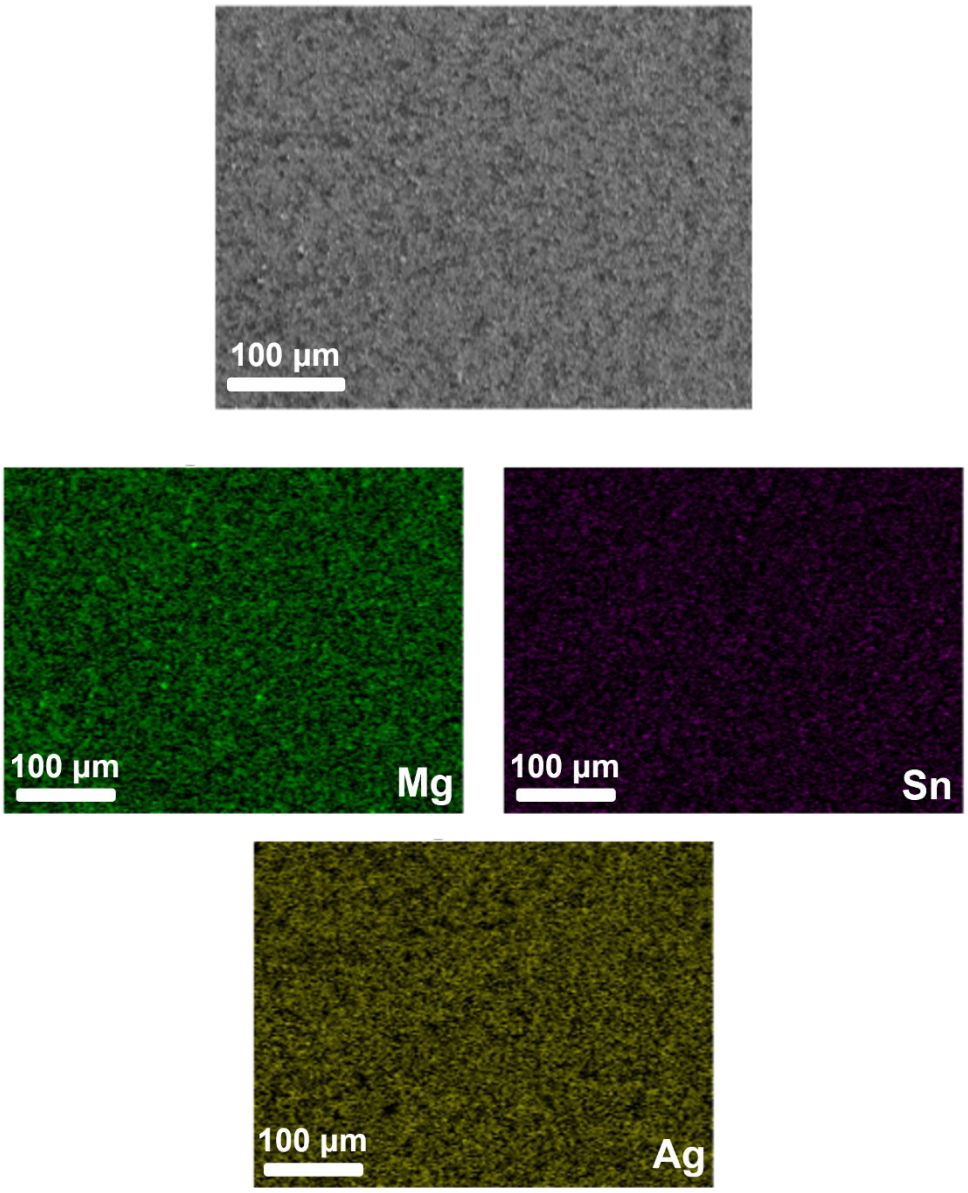

Fig. S2 Top surface SEM-EDS images of the MgAgSn anode-less electrode.

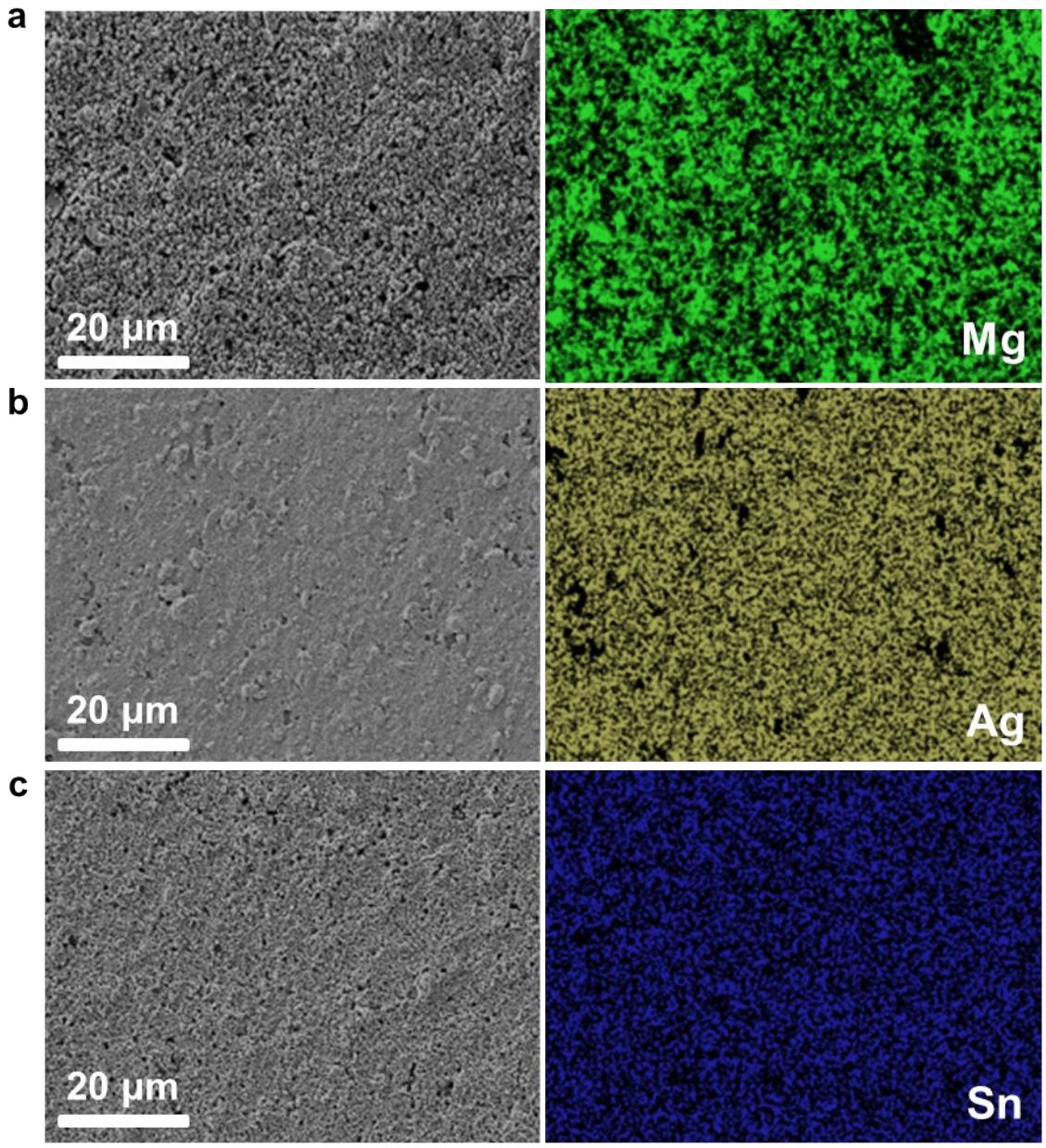

Fig. S3 Top surface SEM-EDS images of the (a) Mg, (b) Ag, and (c) Sn single-seed anode-less electrodes.

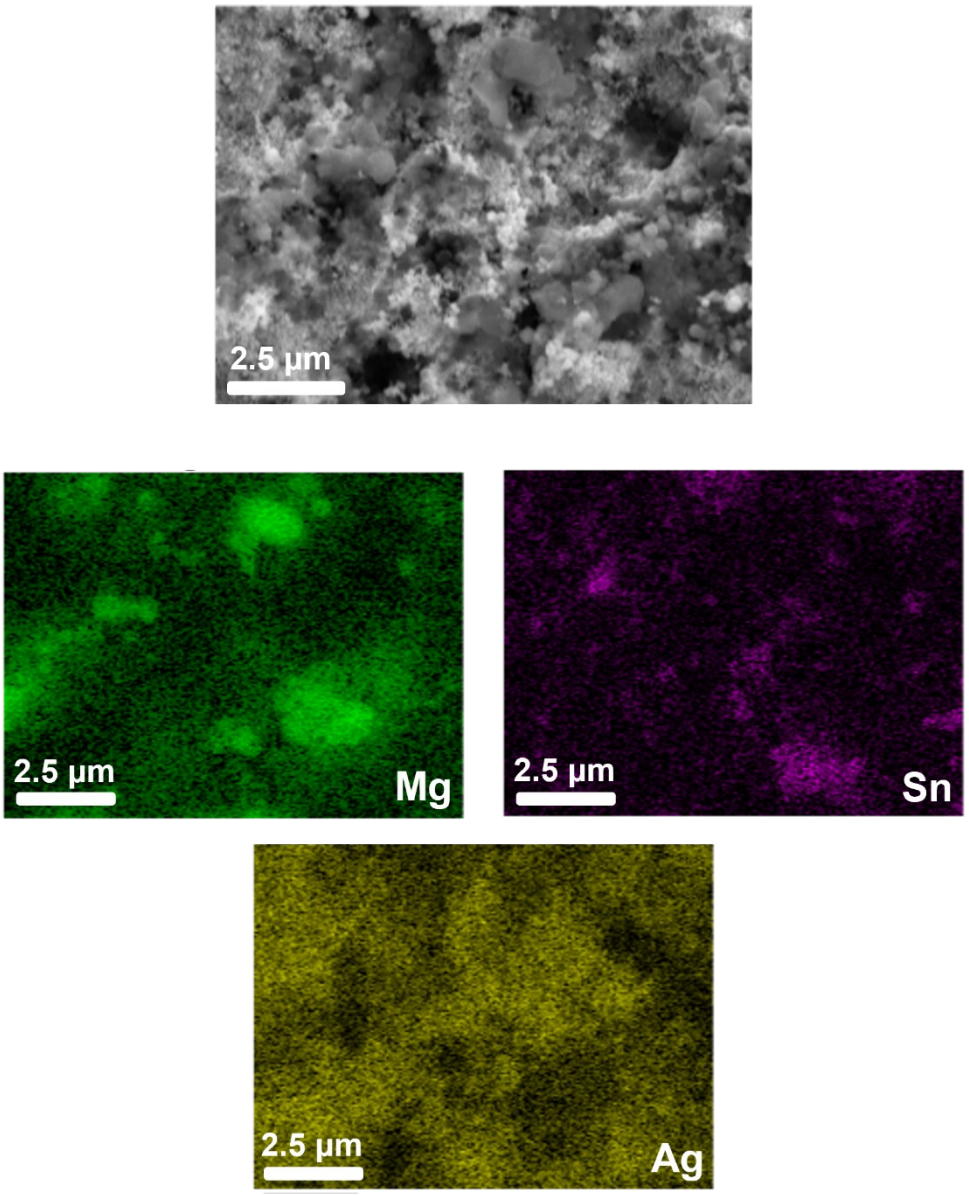

Fig. S4 Highly magnified top surface SEM-EDS images of the MgAgSn anode-less electrode.

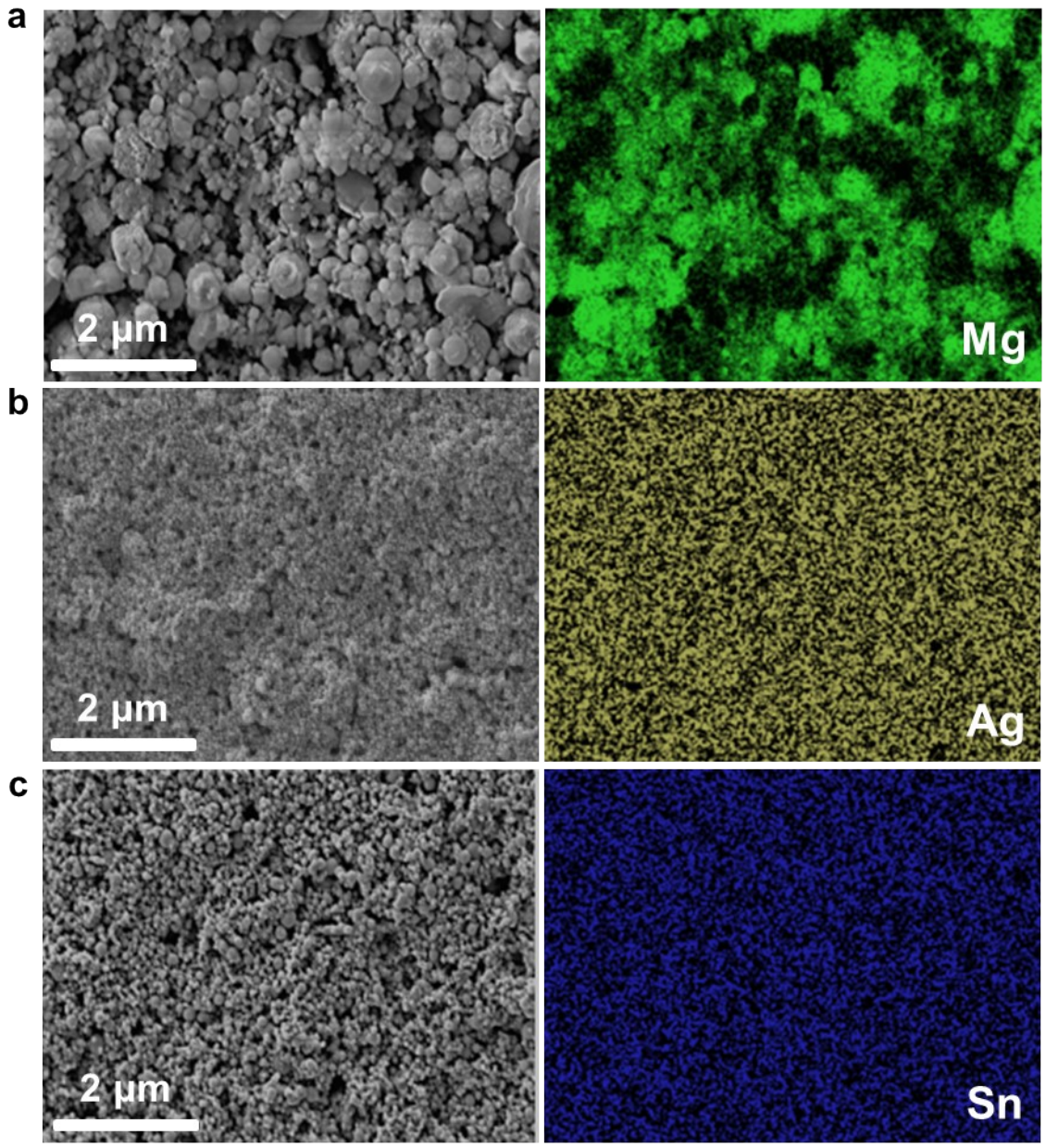

Fig. S5 Highly magnified top surface SEM-EDS images of the (a) Mg, (b) Ag, and (c) Sn single-seed anode-less electrodes.

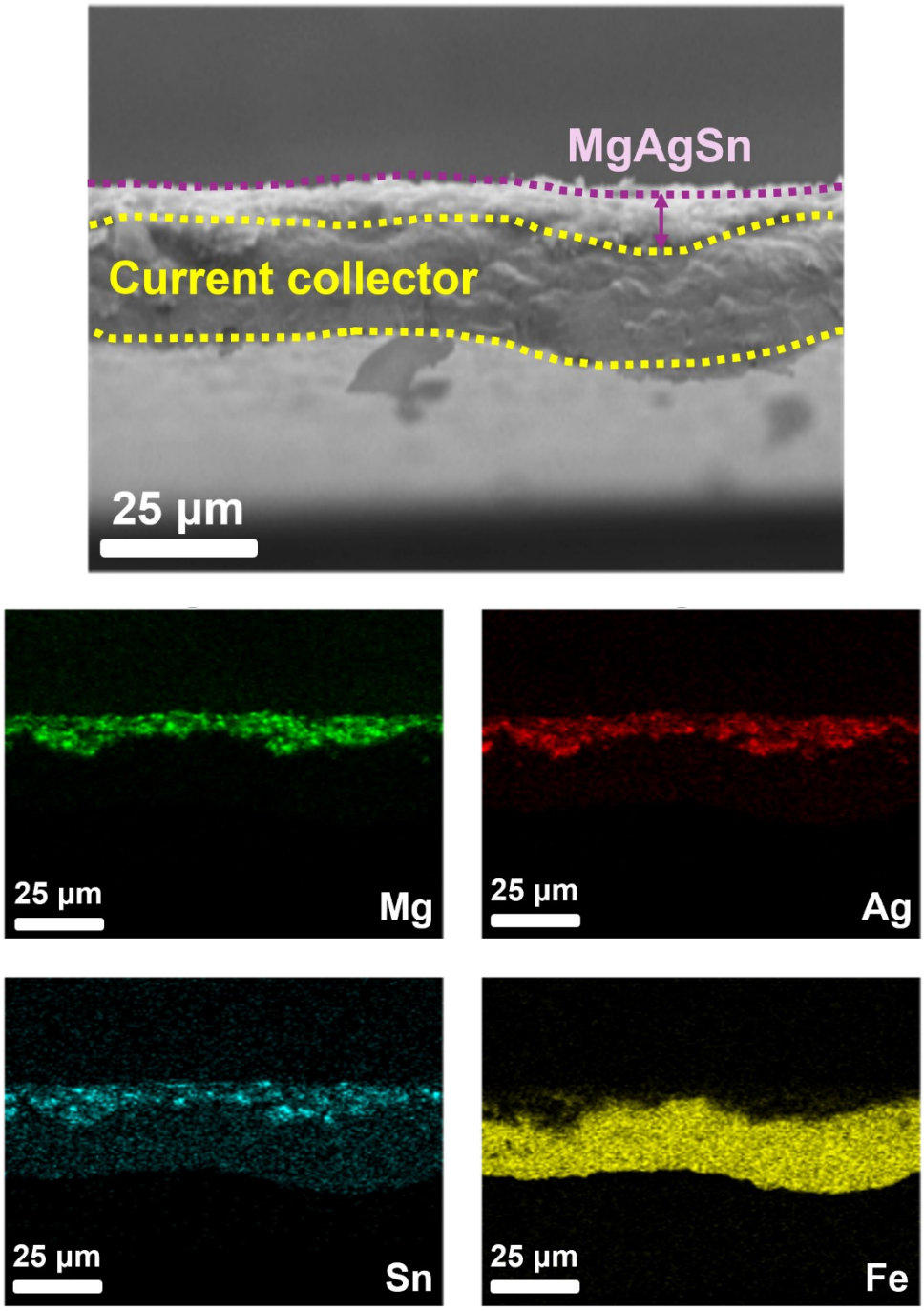

Fig. S6 Cross-sectional SEM-EDS images of the pristine MgAgSn anode-less electrode.

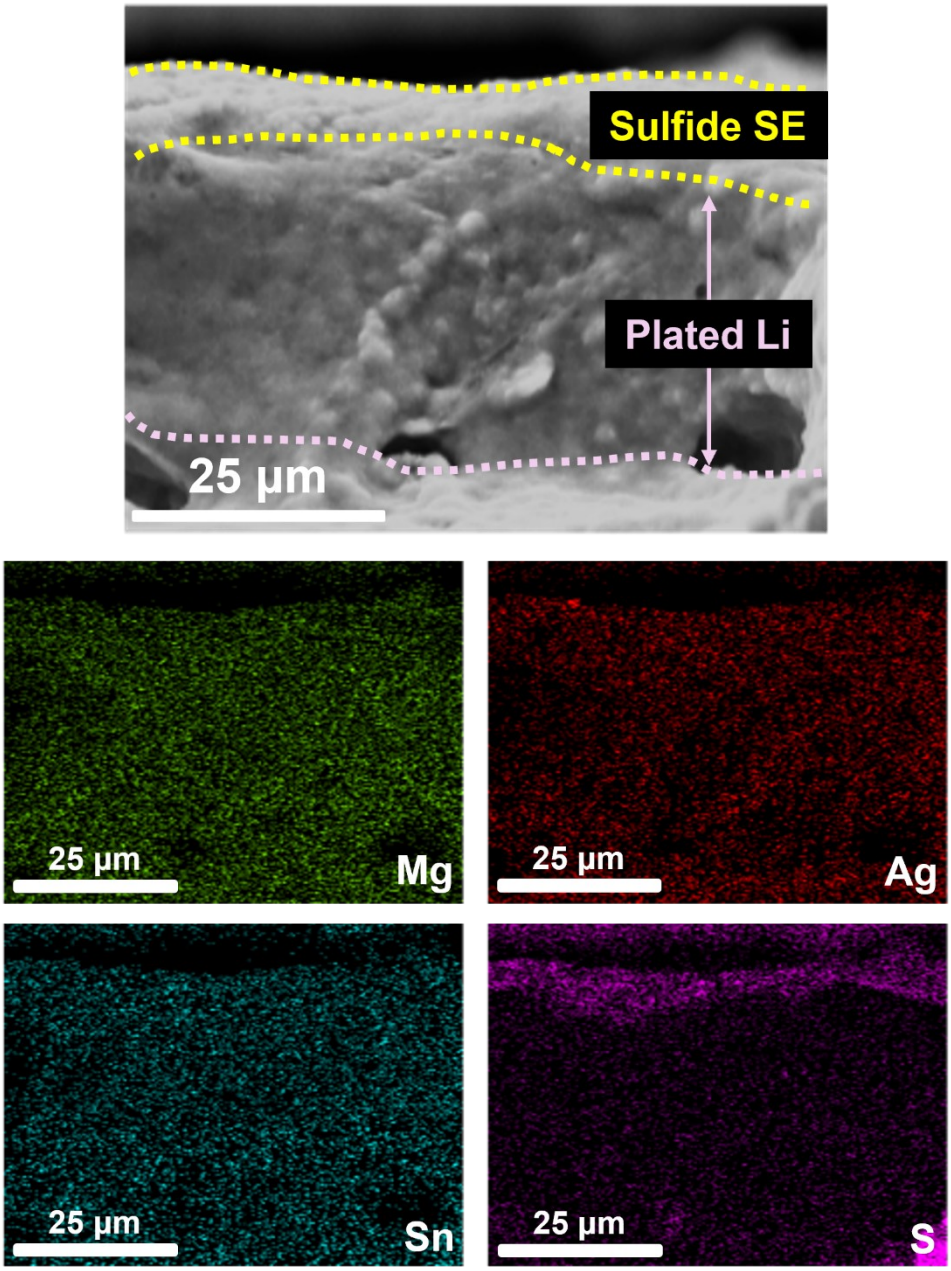

Fig. S7 Cross-sectional SEM-EDS images of the MgAgSn anode-less electrode after the 1st Li plating.

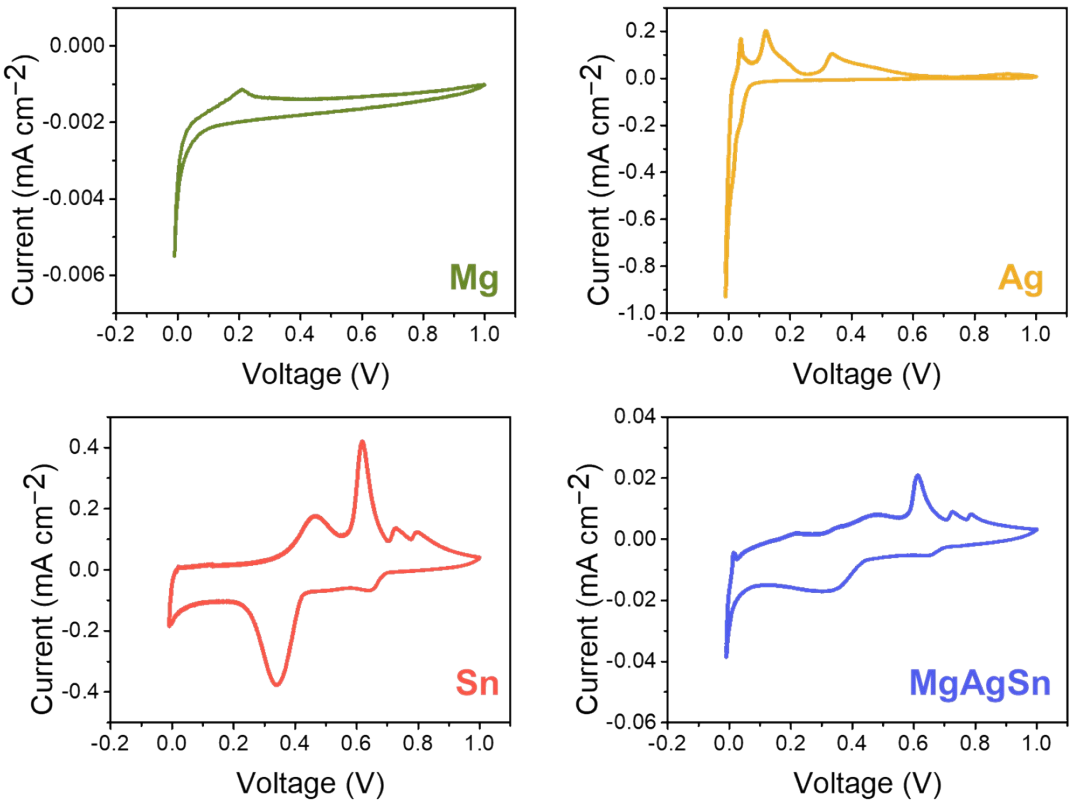

Fig. S8 Cyclic voltammetry (CV) curves of the Mg, Ag, Sn, and MgAgSn-based half-cells.

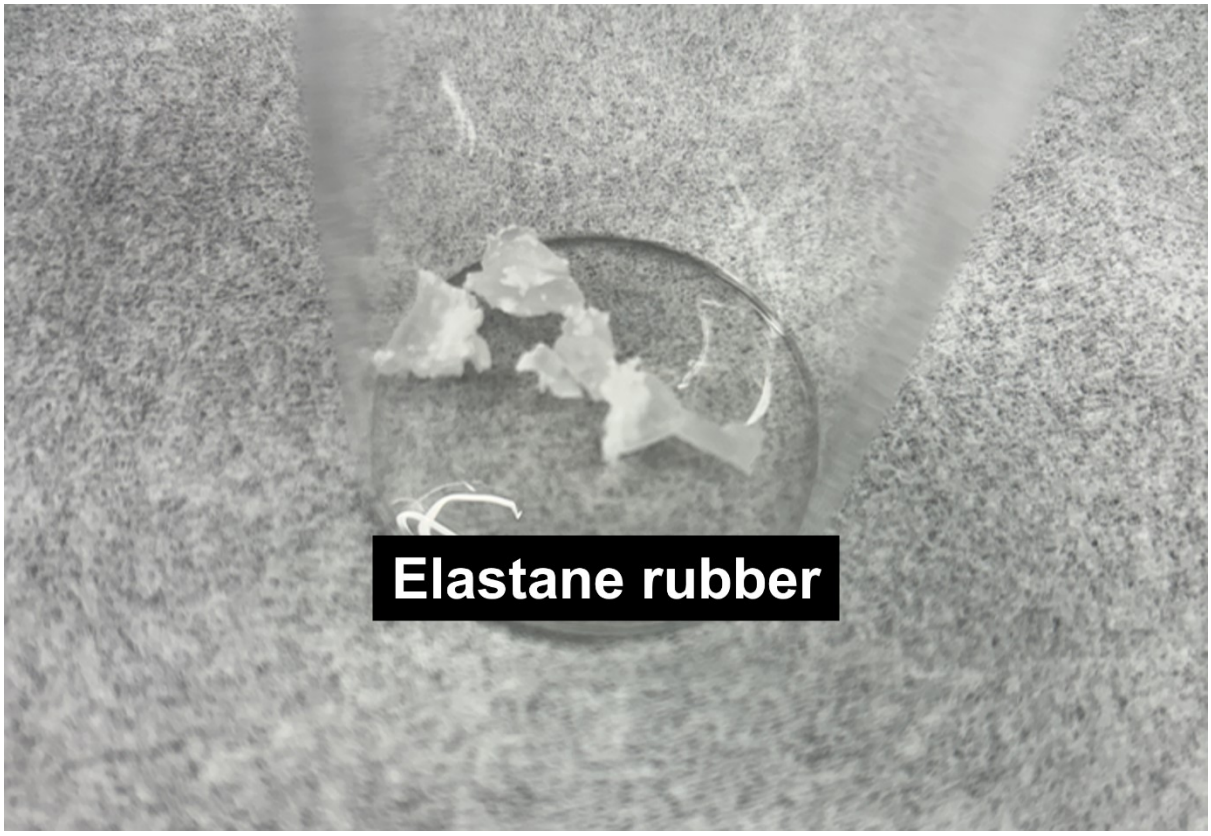

Fig. S9 Photograph of the Elastane rubber.

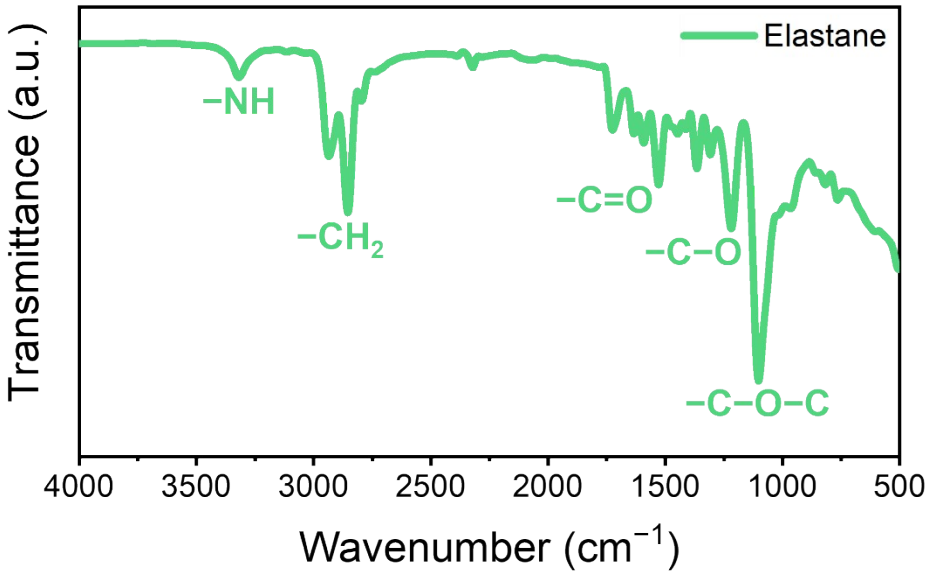

Fig. S10 FT-IR spectra of the Elastane polymer.

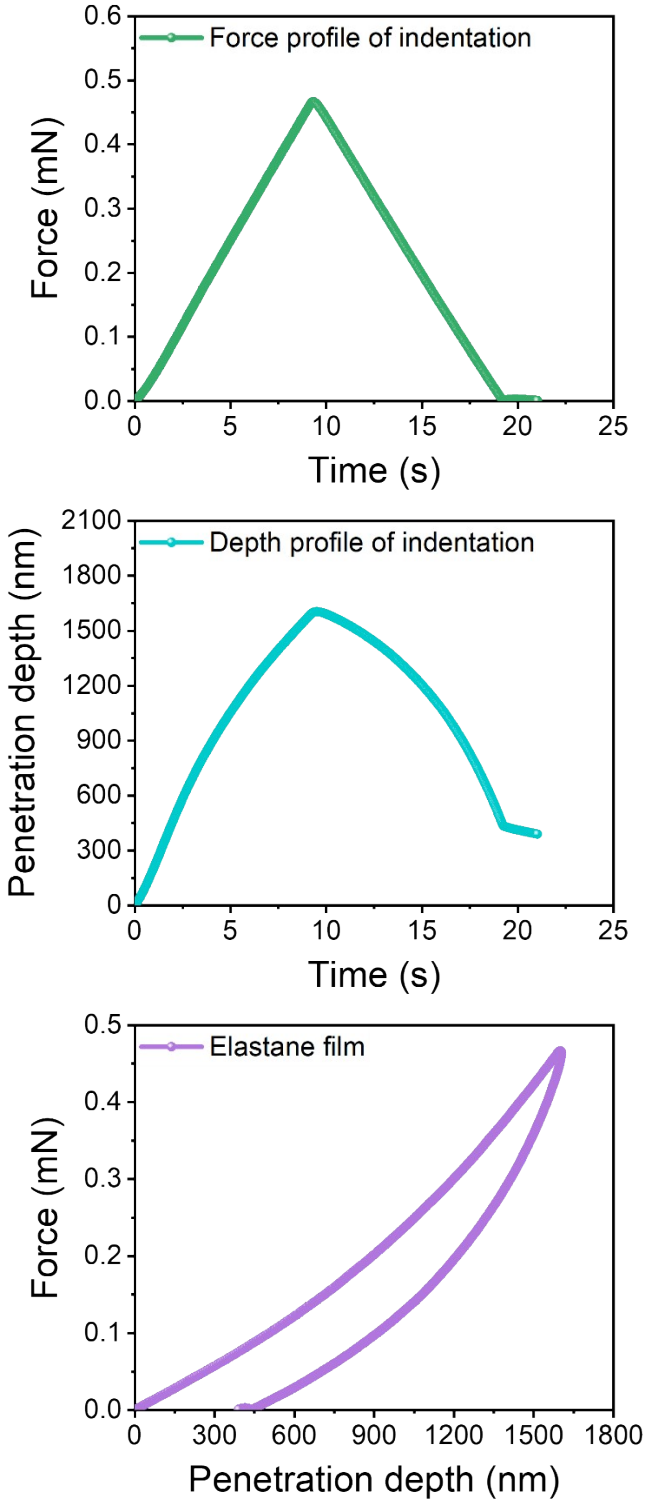

Fig. S11 Nano-indentation profiles of the Elastane polymer film.

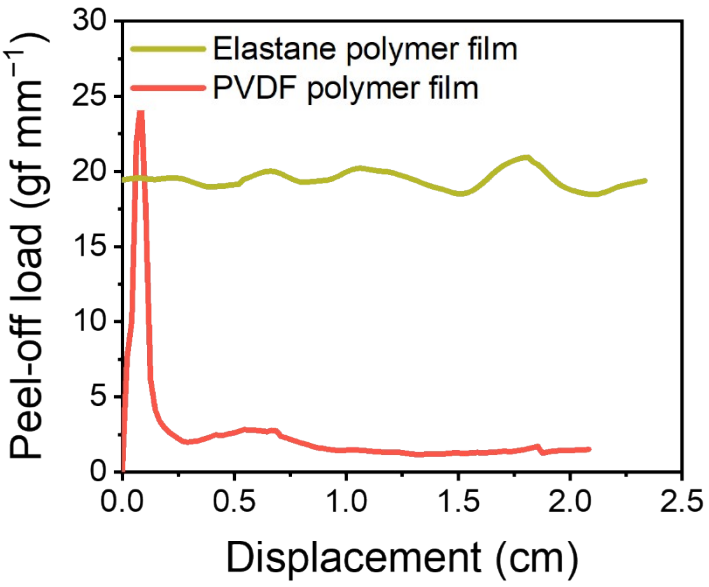

Fig. S12 Peel-off adhesion force test of the polymer films. Both films had the same thickness (15 μm).

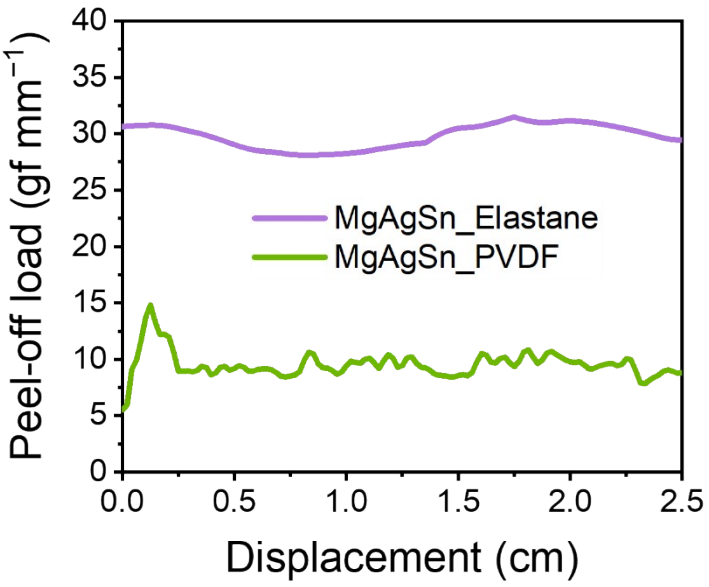

Fig. S13 Peel-off adhesion force test of the MgAgSn anode-less electrodes with the Elastane and PVDF binders.

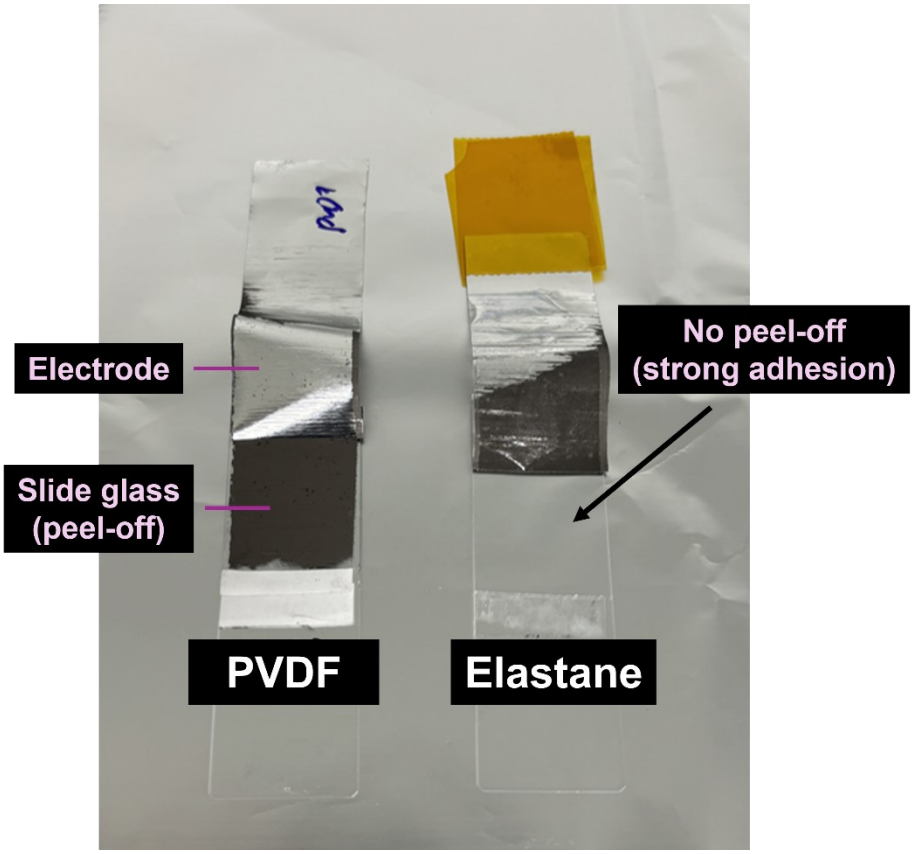

Fig. S14 MgAgSn anode-less electrodes after the peel-off adhesion force test.

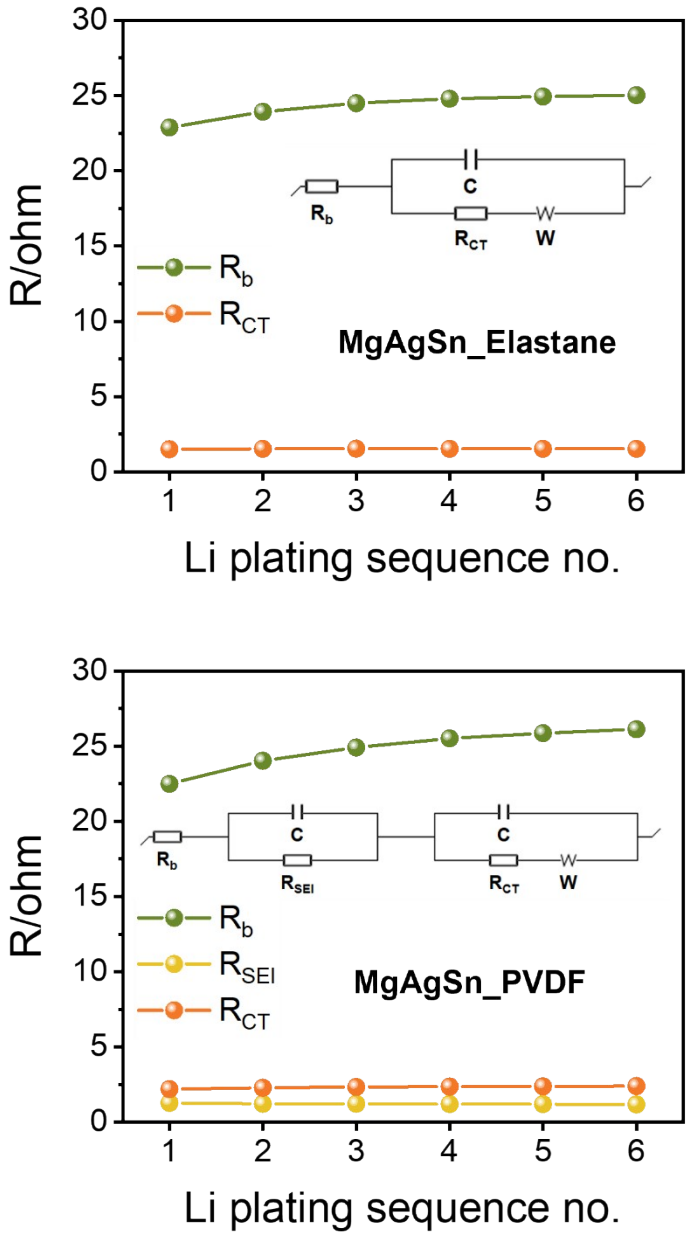

Fig. S15 Resistance values obtained from the in-situ EIS measurements during the Li plating sequences (performed every 10 min at 1 mA cm^{-2}).

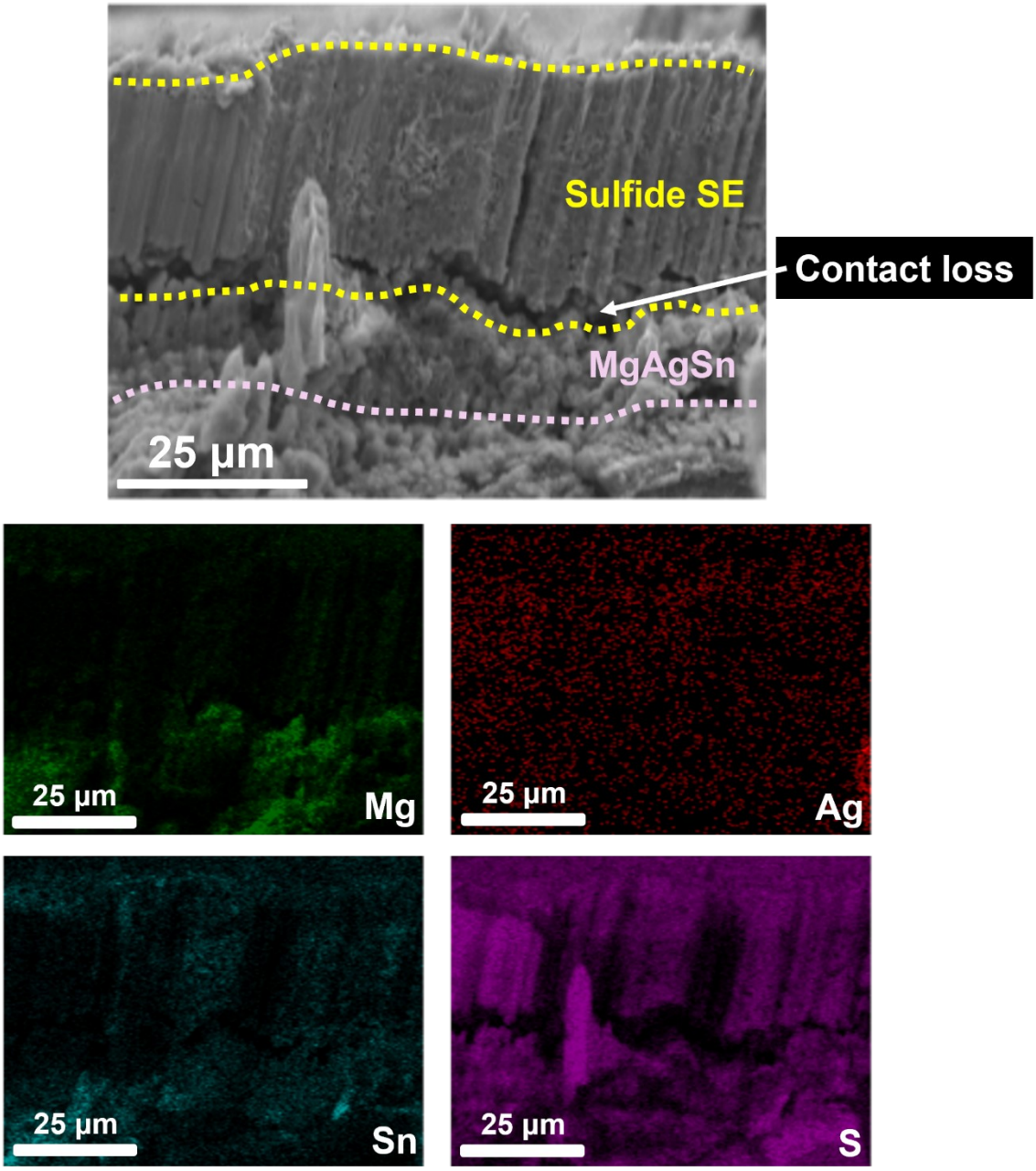

Fig. S16 Cross-sectional SEM-EDS images of the MgAgSn anode-less electrode with the PVDF binder after 50 cycles.

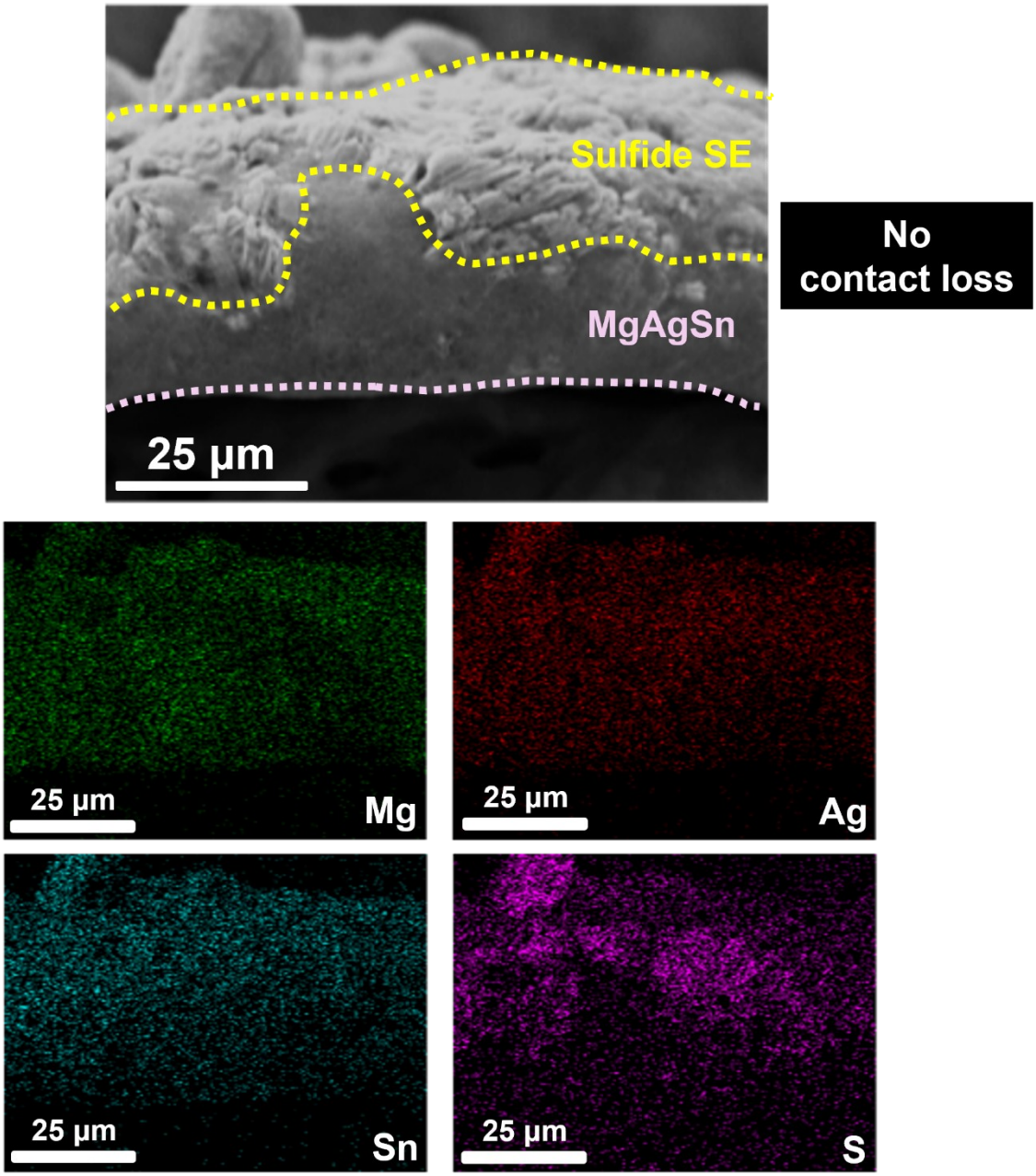

Fig. S17 Cross-sectional SEM-EDS images of the MgAgSn anode-less electrode with the Elastane binder after 50 cycles.

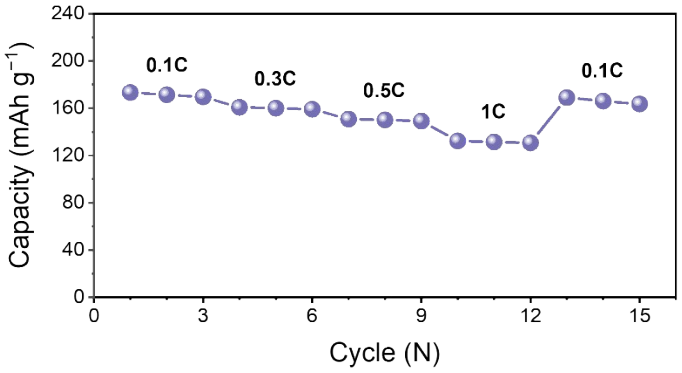

Fig. S18 Rate capability test of full-cell using MgAgSn anode-less electrode with the Elastane binder (1C = 2 mA cm^{-2}).